arXiv:cond-mat/0301554v1 [cond-mat.soft] 28 Jan 2003

Topological Atom Laser

P. Blair Blakie[1,2], Robert J. Ballagh[1] and Charles W. Clark[2]
[1]*Department of Physics, University of Otago, Dunedin, New Zealand and*
[2]*Electron and Optical Physics Division, National Institute of Standards and Technology, Gaithersburg, MD 20899-8410.*

(Dated: February 2, 2008)

We demonstrate how a topological atom laser can be realized by output coupling a trapped vortex state with a Raman scattering process. We find a linearized analytic solution from which a generalized resonance condition for Raman output coupling is developed. Using numerical simulations of a two component Gross-Pitaevskii equation in two and three dimensions the output beam from a trapped central vortex state is analyzed for cases of pulsed and continuous coupling where the vortex core is either transverse or parallel to the direction of propagation. We show how the parameters of the Raman light fields control the spatial phase of the output beam.

PACS numbers: 03.75.Fi

I. INTRODUCTION

One of the most important technological developments to arise to date from dilute gas Bose-Einstein condensation is the atom laser [1, 2, 3, 4, 5]. Analogously to its optical counterpart, the atom laser produces highly coherent, directed matter waves, and properties of this output beam, such as temporal and spatial coherence, and beam divergence have been characterized experimentally [6, 7, 8]. The typical atomic laser configuration uses a confining magnetic potential to act as a cavity for the laser mode, which is occupied by a Bose Einstein condensate. Radio-frequency or optical Raman transitions are then used to coherently transfer atoms into untrapped hyperfine states which can propagate freely away from the remaining trapped atoms [9]. Usually the condensate is taken to be in the ground motional state of its confining potential, though it may possess thermal excitations [10].

In this paper we consider the matter wave output from a condensate in a topologically excited state. To be definite, we take the condensate to be in a central vortex state, though our formalism is sufficiently general to apply to a broader range of topological states including non-stationary states such as vortex arrays [e.g., see [11]]. We present a $T = 0\,\mathrm{K}$ Gross-Pitaevskii treatment of the topological atom laser dynamics, and give numerical results that characterize the behavior over a wide parameter regime, for two different scenarios: pulsed and continuous scattering of the matter field with the output beam direction transverse to the vortex core, and continuous scattering in the direction parallel to the vortex core. We obtain a linearized analytic solution for the output matter wave, and use it to determine the resonance condition for the Raman process and to characterize the phase properties of the atom laser.

II. FORMALISM

A. Raman Coupling

In this paper we consider a Raman output coupling mechanism of the type experimentally demonstrated by Hagley *et al.* [3]. In that scheme the absorption and emission of optical photons from far detuned laser fields coherently transfers atomic population between hyperfine states and imparts sufficient momentum for the output coupled atoms to recoil relative to the trapped condensate.

The ideal situation for an atom laser is to have only two hyperfine states coupled: (1) a weak field seeking state which we label $|1\rangle$ which is magnetically trapped by the confining potential into the laser modes; (2) an untrapped state $|2\rangle$ in which atoms can freely propagate to form a directed output matter wave.

The states $|1\rangle$ and $|2\rangle$ have an energy difference $E_2 - E_1 = \hbar\omega_{21}$, and are coupled through an intermediate state $|e\rangle$ by two laser fields, with frequency ω_1 and wavevector $\mathbf{k}_1$, and frequency ω_2 and wavevector $\mathbf{k}_2$ respectively. The atom makes a transition from state $|1\rangle$ to state $|2\rangle$ by absorbing an ω_1 photon, and emitting an ω_2 photon, thus transferring kinetic energy

$$\hbar\omega \equiv \hbar(\omega_1 - \omega_2) - \hbar\omega_{21} \tag{1}$$

and momentum $\hbar\mathbf{k} = \hbar(\mathbf{k}_1 - \mathbf{k}_2)$ to the atom's center of mass motion. The laser fields are assumed to be sufficiently far detuned from the individual transitions that the effects of spontaneous emission can be ignored, and the laser detunings can be represented by a single value Δ. We can then adiabatically eliminate the intermediate state $|e\rangle$, and represent the laser field coupling between states $|1\rangle$ and $|2\rangle$ by a two photon Rabi frequency $V = \Omega_1\Omega_2^*/2\Delta$, where Ω_j is the single photon Rabi frequency associated with the ω_j radiation field.

The condensate atoms will be scattered into the output state only if the Raman energy transfer is approximately resonant i.e. $\omega \approx \omega_k$ where $\hbar\omega_k = \hbar^2k^2/2m$ is the recoil energy due to the momentum transfer to the atoms. We note that the quadratic dependence of the recoil energy on k makes subsequent Raman transitions into other Zeeman sublevels nonresonant. Thus provided V is small compared to ω_k, any subsequent coupling will be negligible, and the system can be regarded as being effectively two state.

B. Matter Wave Evolution

The condensate atoms in internal state $|1\rangle$ have center of mass wavefunction $\psi_1(\mathbf{r})$ and are trapped in the cavity res-

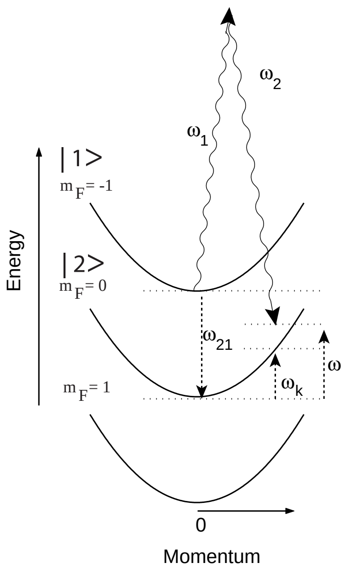

FIG. 1: Raman couplings between internal Zeeman sublevels and momentum states in an $F = 1$ hyperfine manifold, appropriate for Rb^{87} and Na^{23}. The frequencies of the two Raman lasers are ω_1 and ω_2 respectively, and the other quantities are defined in the text.

onator mode by a harmonic potential $V_T(\mathbf{r})$. Correspondingly, the atoms in state $|2\rangle$ have wavefunction $\psi_2(\mathbf{r})$. The stationary modes of the trap (or resonator) satisfy the Gross-Pitaevskii equation

$$\hbar\mu\psi_1 = -\frac{\hbar^2}{2m}\nabla^2\psi_1 + V_T(\mathbf{r})\psi_1 + w|\psi_1|^2\psi_1, \qquad (2)$$

where $\hbar\mu$ is the chemical potential and the collisional interaction strength w is given by $4\pi\hbar^2 a_{11}N_0/m$ with a_{11} the s-wave scattering length for state $|1\rangle$ and N_0 the number of condensate atoms.

For a topological atom laser we require that the trapped condensate is in a topological state, whose properties will be transferred to the output matter wave. For simplicity we consider the case where the initial condition for the condensate is a solution of Eq. (2) that possesses a phase winding: in particular we will assume a central vortex state with a single quantum of circulation.

The time evolution of the trapped condensate and the outcoupled matter fields at $T = 0\,\mathrm{K}$ is given by the coupled Gross-Pitaevskii equations [12]

$$\begin{aligned} i\hbar\frac{\partial\psi_1}{\partial t} &= -\frac{\hbar^2}{2m}\nabla^2\psi_1 + V_T(\mathbf{r})\psi_1 + w(|\psi_1|^2+|\psi_2|^2)\psi_1 \\ &\quad + \frac{\hbar V(t)^*}{2}e^{-i(\mathbf{k}\cdot\mathbf{r}-\omega t)}\psi_2, \qquad (3) \\ i\hbar\frac{\partial\psi_2}{\partial t} &= -\frac{\hbar^2}{2m}\nabla^2\psi_2 + w(|\psi_1|^2+|\psi_2|^2)\psi_2 \\ &\quad + \frac{\hbar V(t)}{2}e^{i(\mathbf{k}\cdot\mathbf{r}-\omega t)}\psi_1, \qquad (4) \end{aligned}$$

We have taken all scattering lengths between and within states to be degenerate, and we note that the normalization condition for the wavefunctions is $\int d\mathbf{r}\ \left[|\psi_1|^2+|\psi_2|^2\right] = 1$. In this paper we solve Eqs. (3) and (4) numerically in two and three spatial dimensions and also obtain an analytic solution for the output wave.

III. LINEARIZED ANALYTIC SOLUTION

We will consider the regime where the depletion of the trapped condensate is negligible on the time scale of the output coupling. This condition will allow us to consider a perturbative solution for the output beam amplitude, valid to first order in V. At this order, we can ignore depletion of the trapped condensate, and write $\psi_1(\mathbf{r},t) = \sqrt{\rho(\mathbf{r})}\exp\left(iS_0(\mathbf{r}) - i\mu t\right)$ where $\rho(\mathbf{r})(=|\psi_1(\mathbf{r},0)|^2)$ and $S_0(\mathbf{r})$ are the density and phase profiles of the initial trapped state respectively. We will also assume that we can neglect the collisional interaction of atoms in state $|2\rangle$ on themselves, and on atoms in state $|1\rangle$. This requires that the density of the scattered atoms is small compared to the trapped atom density in the region of overlap, which is consistent with the negligible depletion assumption. Transforming ψ_2 to an interaction picture (to remove the free particle-like motion) defined as $\psi_2(\mathbf{r},t) = \bar{\psi}_2(\mathbf{r},t)\exp(i\mathbf{k}\cdot\mathbf{r} - i\omega t)$, Eq. (4) can now be written in its linearized form as

$$\begin{aligned} i\hbar\frac{\partial\bar{\psi}_2}{\partial t} &= \left[-\frac{\hbar^2}{2m}\nabla^2 - \hbar\delta - i\hbar\mathbf{K}\cdot\nabla + w\rho(\mathbf{r})\right]\bar{\psi}_2 \\ &\quad + \frac{\hbar V(t)}{2}\sqrt{\rho(\mathbf{r})}e^{iS_0(\mathbf{r})-i\mu t}, \qquad (5) \end{aligned}$$

where $\delta = \omega - \omega_k$ is the Raman detuning from free particle resonance, $\mathbf{K} = \hbar\mathbf{k}/m$ is the recoil velocity, and in accordance with the linearized treatment we have ignored nonlinear terms involving $\bar{\psi}_2$.

If the velocity spread in the trapped condensate is small compared to K then we can ignore the effects of diffusion (about the central momentum $\hbar\mathbf{k}$) of the scattered wave packet by neglecting the Laplacian term in Eq. (5). Noting that the local velocity of the trapped condensate at position $\mathbf{R}$ is

$$\mathbf{v}(\mathbf{R}) = \frac{\hbar\nabla_{\mathbf{R}}S_0(\mathbf{R})}{m}, \qquad (6)$$

this approximation is valid where $\mathbf{v}(\mathbf{R})^2 \ll \mathbf{K}^2$. For typical experimental parameters this condition will be well satisfied everywhere on the trapped condensate except close to the vortex core where the velocity field diverges. Making this approximation we obtain the formal solution for the output coupled wave packet

$$\bar{\psi}_2(\mathbf{r},t) = -\frac{i}{2}\int_0^t ds\, e^{i\Theta(\mathbf{r},t,s)}V(s)\sqrt{\rho(\mathbf{r}+\mathbf{K}(s-t))}, \qquad (7)$$

where

$$\begin{aligned} \Theta(\mathbf{r},t,s) &= S_0(\mathbf{r}+\mathbf{K}(s-t)) - \mu s + (t-s)\delta \\ &\quad - \frac{w}{\hbar}\int_s^t ds'\,\rho(\mathbf{r}+\mathbf{K}(s'-t)). \qquad (8) \end{aligned}$$

In previous work we have presented a similar approximate solution for Bragg scattering (where only a single internal state is involved) and have verified that it provides a good representation of the behavior of the Gross-Pitaevskii equation over a wide parameter regime [13].

The interpretation of Eq. (7) is similar to the Bragg case. As the scattered packet moves across the trapped condensate, the amplitude ψ_2 at a given point (stationary in the frame moving with velocity $\mathbf{K}$) is built up from the sum of contributions coupled in from the trapped condensate at successive points along the trajectory $\mathbf{R} = \mathbf{r} + \mathbf{K}(s - t)$. The contribution coupled into ψ_2 at time s from position $\mathbf{R}$, has moved to position $\mathbf{r}$ at time t and and has acquired a net phase of $\Theta(\mathbf{r}, t, s)$. If the phase term Θ varies sufficiently slowly along a given trajectory, then the cumulative contributions of matter scattered from the trapped condensate will interfere constructively. Maximal scattering occurs when δ is chosen so that there is a point of stationary phase along the trajectory (i.e. $d\Theta(\mathbf{r}, t, s)/ds = 0$), which gives the generalized Raman resonance condition

$$\delta \approx \left[\nabla_{\mathbf{R}} S_0(\mathbf{R}) \cdot \mathbf{K} - \mu + w\rho(\mathbf{R})/\hbar\right]_{\mathbf{R}=\mathbf{r}+\mathbf{K}(s-t)} . \qquad (9)$$

It should be stressed that Eq. (9) is a local condition, which will apply only at certain positions in the condensate. This leads to the important property that the Raman scattering process can be spatially selective. The resonance condition Eq. (9) differs from the Bragg resonance condition we previously derived [12], and gives rise to the following physical interpretation. Immediately after the Raman ejection process, an atom at $\mathbf{R}$ will have velocity $\mathbf{K} + \mathbf{v}(\mathbf{R})$ [see Eq. (6)]. The atom will also have center of mass energy $\hbar(\omega + \mu)$, arising from the chemical potential released from the trapped condensate ($\hbar\mu$), together with an additional energy $\hbar\omega$ gained from the radiation field. This energy is divided between kinetic energy $m(\mathbf{K} + \mathbf{v}(\mathbf{R}))^2/2$ and potential energy $w\rho(\mathbf{R})$ arising from interaction with the atoms remaining in the trapped condensate. Energy conservation during the Raman process is therefore expressed as

$$\hbar(\omega + \mu) = \frac{m}{2}(\mathbf{K} + \mathbf{v}(\mathbf{R}))^2 + w\rho(\mathbf{R}). \qquad (10)$$

One can easily see that Eq. (10) is equivalent to Eq. (9) provided we neglect the term in $\mathbf{v}(\mathbf{R})^2$, consistent with the validity condition $\mathbf{v}(\mathbf{R})^2 \ll \mathbf{K}^2$ used in deriving the analytic solution. It is also convenient below to interpret the term $\nabla S_0 \cdot \mathbf{K}$ as the Doppler shift due to the local velocity of the condensate. Two particular cases of the resonance condition are worth examining:

(i) For a non-interacting ground state (i.e. $S_0 = 0, w = 0$) the resonance condition (9) is $\delta = -\mu$. This is in contrast to the result for Bragg scattering for this case, where resonance is at $\delta = 0$, with the difference due to the fact that the Raman process ejects the atom from the trapped initial state, so releasing the energy of that state.

(ii) For an interacting ground state (i.e. $S_0 = 0$) the resonance condition is $\delta = w\rho(\mathbf{R})/\hbar - \mu$. By density weighting the contributions from all $\mathbf{R}$ across the condensate (assuming a Thomas-Fermi profile) we find that the maximum amount of atoms will be scattered when $\delta = -3\mu/7$.

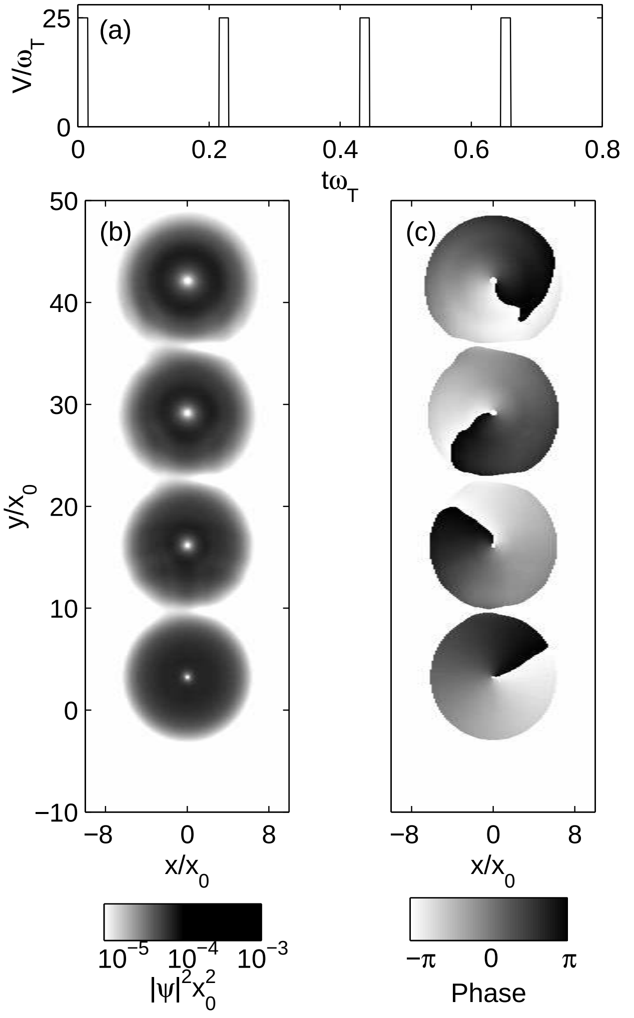

FIG. 2: Pulsed output matter wave from a 2D, $m = -1$, central vortex state in a radially symmetric trap at $t = 0.71t_0$. (a) Temporal dependence of the Raman coupling $V(t)$. (b) Output density profile. (c) Output phase profile. Raman output coupler parameters: $\mathbf{k} = 30\hat{\mathbf{k}}_y/x_0$, $\omega = 925\omega_T$, $\delta = 25\omega_T$, and $V_{\max} = 25\omega_T$. Condensate parameters: $w = 500w_0$ and $\mu = 9.2\omega_T$. Quantities are expressed in harmonic oscillator units with $t_0 = 1/\omega_T$, $x_0 = \sqrt{\hbar/2m\omega_T}$, and $w_0 = \hbar\omega_T x_0^2$, where ω_T is the harmonic trap frequency for the trapped condensate.

IV. PULSED OUTPUT COUPLING

Here we consider a configuration of Raman fields which are pulsed in time with a scattering direction (i.e. $\hat{\mathbf{K}}$) perpendicular to the vortex core. With this choice, one axis of the plane containing the characteristic spatial and phase variations of the vortex is parallel to the direction of the beam propagation. For convenience we present 2D simulations of this geometry with the Raman momentum difference vector along the y-direction, i.e. $\mathbf{k} = k\hat{\mathbf{y}}$. The initial trapped state is assumed to be of the form $\psi_1(x,y) = R(r)e^{i\phi}$, where r and ϕ are the radial coordinate and polar angle respectively.

In Fig. 2 we show the output matter wave (i.e. $\bar{\psi}_2$) after the application of four Raman pulses. The length of each pulse τ_p is chosen to be sufficiently short that the atoms hardly move during the pulse, i.e. $\tau_p \ll R_c/K$ (where R_c is the condensate radius), while the time between pulses is sufficiently long that the scattered atoms can traverse the trapped condensate before the next pulse is applied. The Raman intensity envelope $V(t)$ is shown in Fig. 2(a), and the resulting output coupled density and phase are shown in Figs. 2(b) and (c). It is clear that this procedure produces copies of the trapped vortex state in the output state, including a 2π phase circulation, a result that we confirm analytically below. We note that because $\bar{\psi}_2$ is defined in an interaction picture with respect to the free particle center-of-mass motion, the rapid phase gradient due to the mean wave packet velocity $\mathbf{K}$ has been removed, allowing the phase information in Fig. 2(c) to be more easily discerned. For this reason all the phase plots we show in this paper will be given for the interaction wavefunction.

The Fourier frequency width of each short pulse in our simulation is $\sim 210\,\omega_T$, which is much larger than the typical frequencies associated with meanfield and Doppler shifts. In this transient temporal regime, the resonance condition Eq. (9) is inapplicable, however the frequency spread is still sufficiently narrow that there is no significant coupling into other magnetic sublevels. As long as the central frequency is close to resonance ($\omega \approx \omega_k$) this temporal-limited frequency spread causes the Raman coupling to be resonant everywhere on the trapped condensate facilitating the complete copying of the wavefunction into the output component. The analytic solution Eq. (7) contains the vortex output result of Fig. 2 as we can show by modeling an individual Raman pulse at time t_j as a delta function $V_0\delta(t-t_j)$. For simplicity we shall choose V_0 to be real, and then using Eq. (7) we obtain for $t > t_j$ (in the non-interaction picture)

$$\psi_2(\mathbf{r},t) = -\frac{i}{2}V_0\sqrt{\rho(\mathbf{r}-\mathbf{R}_j)}\exp(i\mathbf{k}\cdot\mathbf{r})\exp(i\,\theta) \qquad (11)$$

where $\mathbf{R}_j = \mathbf{K}(t-t_j)$, and

$$\begin{aligned}\theta &= -\omega t + S_0(\mathbf{r}-\mathbf{R}_j) - \mu t_j + (t-t_j)\delta \\ &\quad -\frac{w}{\hbar}\int_{t_j}^{t} ds'\,\rho(\mathbf{r}+\mathbf{K}(s'-t)). \end{aligned} \qquad (12)$$

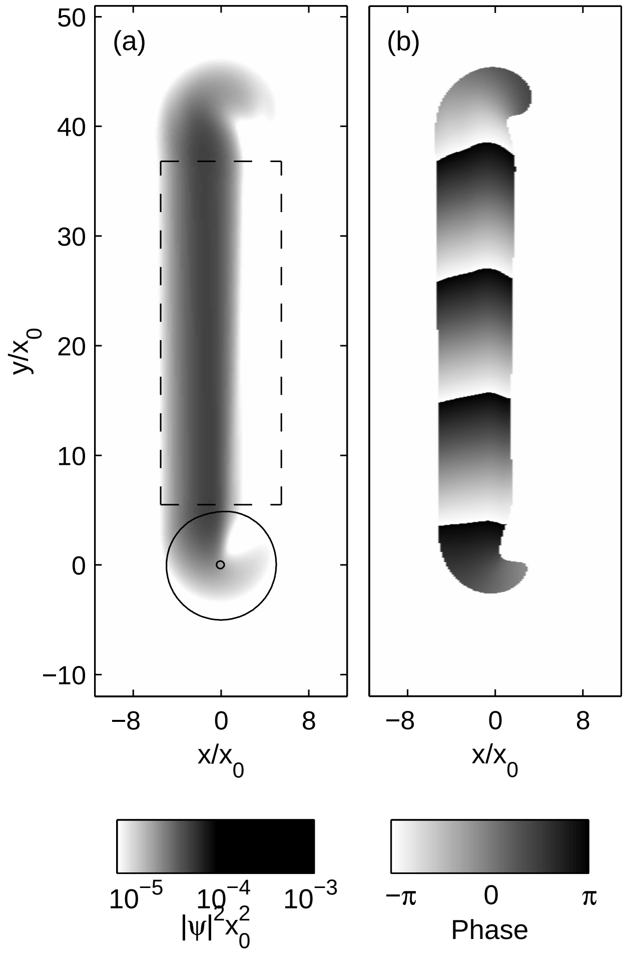

FIG. 3: Continuously output coupled matter wave from a 2D, $m = -1$, central vortex state of a radially symmetric trap at $t = 0.71t_0$. with continuous Raman coupling. (a) Density profile. Dashed line indicates steady state beam region (see text). The solid lines indicate density contours of the trapped vortex state. (b) Phase profile. Raman parameters: $V = 2$, $\omega = 925\omega_T$, $\mathbf{k} = 30\hat{\mathbf{k}}_y/x_0$ and $\delta = 25\omega_T$. Condensate parameters: $w = 500w_0$ and $\mu = 9.2\omega_T$.

The density distribution of the output field in Eq. (11) is the same as the initial vortex state, but displaced by $\mathbf{R}_j$ (and multiplied by $V_0/2$). The phase θ of the field can be written

$$\begin{aligned}\theta &= [S_0(\mathbf{r}-\mathbf{R}_j) - \mu t_j] - \omega t_j - \omega_k\,(t-t_j) \\ &\quad -\frac{w}{\hbar}\int_{t_j}^{t} ds'\,\rho(\mathbf{r}+\mathbf{K}(s'-t)) \end{aligned} \qquad (13)$$

which has the following interpretation. The term in square brackets represents the phase of the trapped vortex at time t_j , which is transferred to the output vortex along with the phase of the Raman coupling (ωt_j) at the time of the pulse. In the absence of collisional interactions the vortex would behave as a free particle of momentum $\mathbf{k}$, and energy ω_k (we have neglected diffusive kinetic energy) and its phase would increment as $\omega_k\,(t-t_j)$. The integral term in Eq. (13) represents the correction to the free particle evolution during the time the output field is transiting the trapped vortex. Notice that the integrand cuts off once $|\mathbf{r}+\mathbf{K}(s'-t)| > R_c$, so that this contribution to the phase becomes constant once the output vortex has separated from the initial vortex. The rotation of the line of zero phase between successive vortices in Fig. 2(c) is thus described by the first 3 terms of Eq. (13).

V. CONTINUOUS OUTPUT COUPLING

In Fig. 3 we show the output matter wave following the application of a long duration, low intensity Raman pulse to a vortex state - which we will refer to here as continuous output coupling. This result displays typical behavior of the scattered solution in the continuous regime: the matter wave is preferentially scattered from a selected spatial region of the trapped condensate and has an asymmetric density distribution transverse to the direction along which it propagates. The shape of the output density profile depends on the detuning δ, and by suitably adjusting this parameter, matter can be selectively coupled out from either side of the trapped vortex. Here the frequency width of the finite duration Raman pulse is sufficiently narrow that the generalized resonance condition (9) is applicable. From this resonance condition, the spatial asymmetry of the output density profile can be understood as arising from the Doppler term $\nabla_{\mathbf{R}} S_0(\mathbf{R}) \cdot \mathbf{K}$. A unit circulation central vortex state with angular momentum number $m = \pm 1$ has a phase profile of the form $S_0 = \pm\phi$, where ϕ is the azimuthal angle. The Doppler effect gives a local shift of the resonant frequency; on the side of the vortex where the current flow runs parallel to the scattering direction the resonant frequency is shifted upward, while on the other side the flow is anti-parallel and the frequency is shifted downward. By choosing δ above or below the central resonance value, it is possible to selectively scatter from either side of the vortex.

To investigate the properties of the continuously output matter wave in more detail we consider the steady state region of the output coupled matter wave. This region, which we indicate pictorially in Fig. 3(a), is where the output beam has constant transverse density profile, that we shall refer to as the *steady state beam profile*. From the formal solution of Eq. (7) it can be shown that for two points $\mathbf{r}$ and $\mathbf{r} + \alpha\mathbf{K}$, both within the steady state beam region, then the values of the wavefunction at these points are related by

$$\bar{\psi}_2(\mathbf{r} + \alpha\mathbf{K}, t) = \bar{\psi}_2(\mathbf{r}, t) e^{i(\delta+\mu)\alpha}. \tag{14}$$

This result indicates that the steady-state velocity of the output matter wave is $\mathbf{K} + \mathbf{V}_0$, where we define

$$\mathbf{V}_0 = \frac{\hbar}{m} \frac{\delta + \mu}{K} \hat{\mathbf{K}}. \tag{15}$$

Remarkably, this is uniform across the transverse profile, a result we can understand using Eq. (9), which shows that at the position where the Raman transfer takes place, the trapped condensate has a local velocity component parallel to $\mathbf{K}$ given by

$$\mathbf{v}(\mathbf{R})_{\parallel} = \frac{\hbar}{m} \frac{(\delta + \mu - w\rho(\mathbf{R}))}{K} \hat{\mathbf{K}}. \tag{16}$$

The velocity of the atom (in direction $\hat{\mathbf{K}}$) immediately after the Raman transfer is therefore $\mathbf{K} + \mathbf{v}(\mathbf{R})_{\parallel}$. We showed in section III that this local ejection velocity gives a kinetic energy consistent with an atom residing in a potential of $w\rho(\mathbf{R})$, (due to the trapped condensate atoms). Once the atom has moved away from the condensate, this potential energy is converted to kinetic energy, consistent with an atom of velocity $\mathbf{K} + \mathbf{V}_0$. We note that the transverse components of the local ejection velocity cancel out in the final scattered wave, due to the symmetry of the vortex velocity distribution. For a general straight-line trajectory across the vortex, there are two positions of local resonance with the same density $\rho(\mathbf{R})$, but with opposite transverse local velocities. It is also worth emphasizing that the control available over the output matter wave velocity is in contrast with the case of optical lasers, where the group velocity of the light cannot be altered without changing the properties of medium in which it propagates.

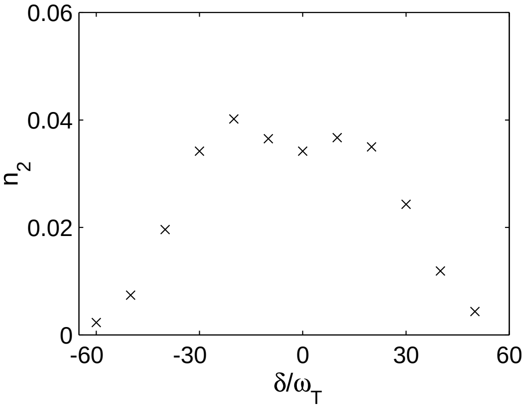

FIG. 4: Population scattered into an output matter wave from a vortex after excitation by a continuous Raman pulse of duration $t = 0.71t_0$. Raman parameters: $\mathbf{k} = 30\hat{\mathbf{k}}_y/x_0$ and $V = 2\omega_T$. Condensate parameters: $w = 500w_0$ and $\mu = 9.2\omega_T$.

We have numerically verified that Eq. (14) is in good agreement with numerical simulations of the Gross-Pitaevskii Equation over a wide regime. We note that changing the Raman detuning δ to control the phase gradient of the output coupled beam also affects the efficiency at which the atoms are scattered, and to characterize this we show the scattered population, i.e. $n_2 = \int d\mathbf{r} |\bar{\psi}_2(\mathbf{r}, t)|^2$ in Fig. 4. This result shows that in this case the frequency width of the Raman coupling (from $\delta \sim -30\omega_T$ to $30\omega_T$) is sufficient to allow the output velocity to be changed over a range of $1.0x_0\omega_T$ without significant attenuation of the output matter wave. In these results the Doppler effect is the dominant broadening mechanism, so that the approximate width of the Raman transition, $\Delta\omega$, will be

$$\Delta\omega = \frac{k\Delta p}{m}, \tag{17}$$

where Δp is the momentum width of the condensate in the scattering direction. For the results in Fig. 4 Eq. (17) gives the full width at half maximum $\Delta\omega = 60.8\omega_T$, where Δp is numerically evaluated from the initial vortex eigenstate (the initial state for ψ_1).

Additionally, it should be noted that the scattered population (n_2) is a convenient experimental observable for measuring the linear response of the condensate to the perturbing

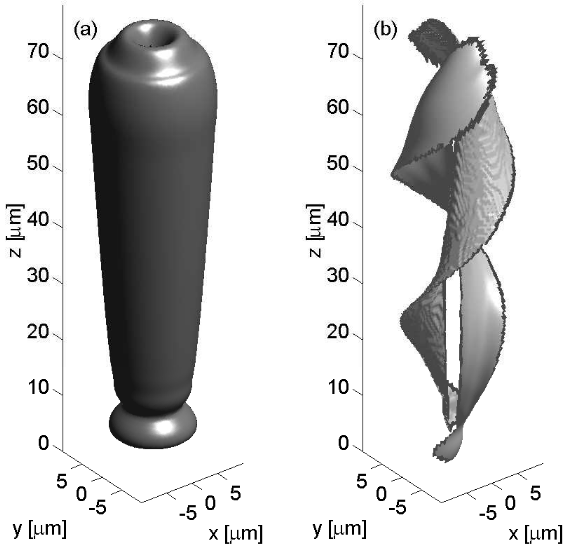

FIG. 5: Output matter wave at $t = 1.4$ms from a 2.2×10^5 atom ^{23}Na condensate in a $m = 1$ central vortex state with $\mu = 1.15$kHz in a spherically symmetric trap of frequency 80Hz. Raman output coupler corresponds to 589nm laser fields at 120° with $\delta = 0$ and a two-photon Raman frequency of $V = 2\pi \times 480\text{s}^{-1}$. (a) 3.4×10^{12}atom/cm^3 density iso-surface of the output matter wave. (b) 0 and π phase iso-surfaces of the output matter wave.

Raman potential. This technique for probing the condensate is similar to Bragg spectroscopy, which was first used on condensates by Stenger *et al.* [14], except that for the Raman case the condensate is scattered into a different internal state. This technique has several advantages over Bragg spectroscopy for conducting high precision measurements of condensate properties which we will explore elsewhere.

Finally we consider continuous output coupling of a central vortex in a direction parallel to the vortex core. Because this arrangement has the superfluid current flow perpendicular to $\mathbf{K}$, the Doppler term and hence the output coupling is not spatially selective[17]. This means that the vortex profile will be reproduced as the transverse profile of the atom laser output, so that the atom laser will have a similar intensity and phase profile to that of a TEM$^*_{01}$ mode of an optical laser, commonly known as the donut mode [16].

In Figs. 5 (a) and (b) we show phase and density iso-surfaces of a vortex output-coupled in the manner described above, for realistic experimental parameters. The noticeable beam divergence in the stable beam region, which extends from about $z = 10\mu$m to $z = 60\mu$m, is enhanced by the centrifugal forces of the rotating condensate beyond that expected simply from repulsive wave packet spreading

The helicity of the phase iso-surface arises from the addition of the phase gradient along the propagation direction (due to the Raman output coupling) to the vortex-like phase profile the matter wave has in the transverse direction. The phase gradient of the matter wave and hence the phase helicity is controlled by Raman detuning, as given in Eq. (14). We have numerically verified that for a case with the same parameters as in Fig. 5, except using $\delta \sim -\mu$, the helicity disappears as the phase iso-surfaces are approximately vertical. Also for $\delta < -\mu$ the helicity changes sign corresponding to the phase iso-surfaces spiraling in the opposite sense.

The helical structure of the phase could be investigated by an interference experiment, such as superimposing the topological atom laser beam with a co-propagating plane phase atom laser.

VI. CONCLUSION

In this paper we have introduced the idea of a topological atom laser and considered its behavior using numerical and analytic approaches over a broad parameter regime. We have developed a linearized solution for the output coupled matter wave from which we have determined a spatially dependent resonance condition for Raman scattering and characterized how the output beam phase properties relate to the Raman detuning and the condensate chemical potential.

VII. ACKNOWLEDGMENTS

This work was supported by the US Office of Naval Research, the Advanced Research and Development Activity. PBB and RJB acknowledge support from the Marsden Fund of New Zealand under contracts PVT902 and PVT202.

---

[1] M.-O. Mewes, M. Andrews, D. Kurn, D. Durfee, C. Townsend, and W. Ketterle, Phys. Rev. Lett. **78**, 582 (1997).
[2] B. Anderson and M. Kasevich, Science **282**, 1686 (1998).
[3] E. Hagley, L. Deng, M. Kozuma, J. Wen, K. Helmerson, S. Rolston, and W. Phillips, Science **283**, 1706 (1999).
[4] I. Bloch, T. W. Hänsch, and T. Esslinger, Phys. Rev. Lett. **82**, 3008 (1999).
[5] J. Martin, C. McKenzie, N. Thomas, J. Sharpe, D. Warrington, P. Manson, W. Sandle, and A. Wilson, J. Phys. B **32**, 3065 (1999).
[6] M. Köhl, T. Hänsch, and T. Esslinger, Phys. Rev. Lett. **87**, 160404 (2001).
[7] M. Trippenbach, Y. Band, M. Edwards, M. Doery, P. Julienne, E. Hagley, L. Deng, M. Kozuma, K. Helmerson, S. Rolston, et al., J. Phys. B **33**, 47 (2000).
[8] Y. L. Coq, J. H. Thywissen, S. A. Rangwala, F. Gerbier, S. Richard, G. Delannoy, P. Bouyer, and A. Aspect, Phys. Rev. Lett. **87**, 170403 (2001).
[9] R. Ballagh and C.M.Savage, in *Proceedings of the Thirteenth Physics Summer School: Bose-Einstein Condensation: Atomic Physics to Quantum Fluids*, edited by C. Savage and M. Das (World Scientic, Singapore, 2000).

[10] S. Choi, Y. Japha, and K. Burnett, Phys. Rev. A **61**, 063606 (2000).
[11] K. Madison, F. Chevy, W. Wohlleben, and J. Dalibard, Phys. Rev. Lett. **84**, 806 (2000).
[12] M. Edwards, D. A. Griggs, P. L. Holman, C. W. Clark, S. Rolston, and W. Phillips, J. Phys. B **32**, 2935 (1999).
[13] P. B. Blakie and R. J. Ballagh, Phys. Rev. Lett. **86**, 3930 (2001).
[14] J. Stenger, S. Inouye, A. Chikkatur, D. Stamper-Kurn, D. Pritchard, and W. Ketterle, Phys. Rev. Lett. **82**, 4569 (1999).
[15] P. Blakie and C. W. Clark (2002).
[16] A. Siegman, *Lasers* (University Science Books, 1986).
[17] There is a residual resonance shift due to the inhomogeneous meanfield, but we have found that typically this does not give rise to significant spatial selectivity if the condensate chemical potential is of order or smaller in size that the Doppler width (see Eq. (17)).